DOI: 10.1002/ejic.201000679

Domination of Local Environment Over Pore Confinement Effects on the Catalytic Performances of Single-Site Cp*Ir^{III}-NHC Heterogeneous vs. Homogeneous H/D Exchange Catalysts

Tarun Kumar Maishal,[a] Malika Boualleg,[a] Mohamed Bouhrara,[a] Christophe Copéret,[a] Erwan Jeanneau,[b] Laurent Veyre,[a] and Chloé Thieuleux*[a]

Keywords: Iridium / Mesoporous materials / Heterogeneous catalysis / Homogeneous catalysis / C-H activation

Three different tailored mesostructured hybrid organic-inorganic materials containing single site Ir–NHC moieties (NHC = N-heterocyclic carbene) were synthesized by a very convenient and attractive methodology: (i) the synthesis of mesostructured materials with different pore-sizes and containing two types of imidazolium units regularly distributed along their channel pores was achieved using a sol-gel process via a templating route; (ii) the in situ transformation of the imidazolium moieties to Ag–NHC units was quantitatively performed; (iii) the transmetallation of Ag–NHC groups with $[Cp^*IrCl_2]_2$ was carried out successfully. Each step was controlled fully and evaluated by several analytical techniques (XRD, N_2 adsorption, elemental analysis, and solid state NMR). The catalytic properties of the resulting Ir–NHC-containing materials were studied in H/D-exchange reactions with various substrates, and compared to their homogeneous homologues. Their catalytic activity highlighted the following: (i) the substituents on the NHC ring have an important role; (ii) the size of the pores have no influence on the catalytic reactivity; (iii) the close environment around the metal center has a major influence on the catalytic reaction. This latter point suggests that the selective C–H bond activation by mesoporous catalysts with a mixture of reagents can be performed by fine tuning the steric hindrance around the metal centers, while keeping big pores for easy of diffusion of substrate and product molecules.

Introduction

The introduction of NHCs as an alternative to phosphanes has led to major breakthroughs, for instance in the areas of olefin-metathesis, C–C coupling and telomerization.[1–5] In recent years, Ir-mediated reactions have been explored in the area of homogeneous catalysis.[6–8] Indeed, of the many catalytic reactions recently reported using iridium complexes C–H activation is quite promising because of its application in making isotopically labeled compounds.[9] While the advantages of heterogeneous over homogeneous catalysts are very well accepted (ease of handling, higher stability, and recyclability), the preparation of supported catalysts that show comparable performances to their homogeneous homologues is still a challenge. We have recently reported an original methodology, based on the synthesis of hybrid organic-inorganic mesostructured materials by a templating route,[12–13] for the preparation of a well defined M–NHC-containing materials that fulfilled the aforementioned requirements (M = Ru,[10] Ir[11]). The intermediate compounds in the synthesis of Ir–NHC contained regularly distributed chlorobenzyl groups that were transformed quantitatively to Ir–NHC moieties; because this material contained regularly distributed well defined Ir–NHC centers, this approach represents a very attractive route for the preparation of well-defined heterogeneous catalysts that could be termed "single-site" catalysts. Herein, we investigate the key factors that influence the C–H bonds activation for several classical substrates, specifically looking at the following parameters: pore diameters, local steric hindrance around the Ir metal center, and substituents on the NHC units.

Results and Discussion

We have prepared different types of mesostructured materials with the following common characteristics (Scheme 1): the same pore network structure (2D hexagonal), a similar texture (surface area, porous volume), and the same concentration and nature of tether (benzyl groups). In addition the materials have specific characteristics: two different pore sizes and two different initial organic groups, namely, $\mathbf{P_3}$ [BJH (Barret–Joyner–Halenda) pore diameter: 3.5 nm, and containing imidazole benzyl groups] and $\mathbf{P_6}$ (BJH pore diameter: 6 nm, and containing chlo-

[a] Université de Lyon, Institut de Chimie de Lyon, UMR 5265 LC2P2 CNRS–Université Lyon 1–ESCPE Lyon,
43, Bd. du 11 Novembre 1918, 69616 Villeurbanne, France
Fax: +33-4-72431795
E-mail: thieuleux@cpe.fr
[b] Centre de Diffractométrie Henri Longchambon-Université Lyon 1,
43, Bd. du 11 Novembre 1918, 69616 Villeurbanne, France
Supporting information for this article is available on the WWW under http://dx.doi.org/10.1002/ejic.201000679.

robenzyl groups). Transformation of $\mathbf{P_3}$ and $\mathbf{P_6}$ into Ir–NHC materials yielded methyl and mesityl-substituted Ir–NHC complexes, respectively, which are denoted as follows: $\mathbf{P_3}$**-Me**, $\mathbf{P_6}$**-Me** and $\mathbf{P_6}$**-Mes**.

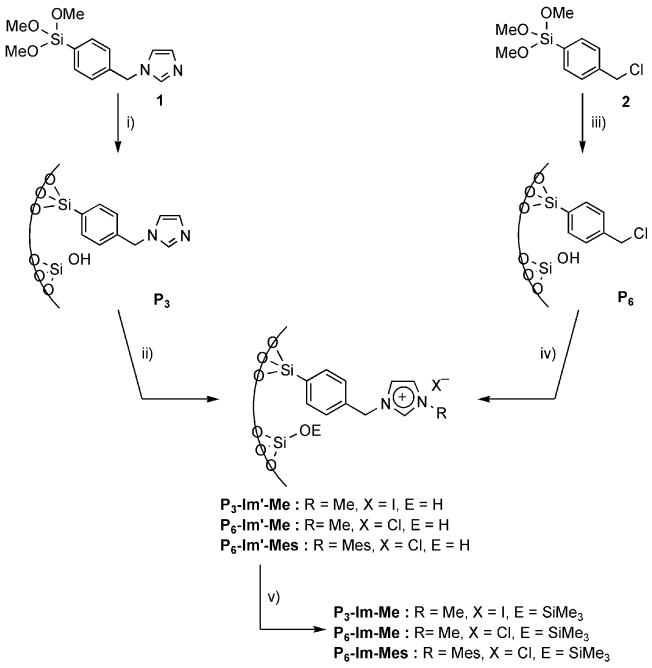

Scheme 1. Synthesis of imidazolium-based hybrid materials with different pore sizes. Reagents: (i) tetraethyl orthosilicate (TEOS), NH_4OH, H_2O, and monohydrated hexadecylpyridinium chloride ($HDPyCl{\cdot}H_2O$), 80 °C, 48 h, followed by the additon of 2 M HCl/H_2O and heating at 45 °C for 2 h; (ii) CH_3I, 50 °C, 24 h; (iii) TEOS, HCl, Pluronic P123, and NaF, 45 °C, followed by the addition of 2 M HCl/H_2O and heating for 2 h at 45 °C; (iv) Mesitylimidazole and toluene, reflux for 2 d for P_6-Im-Mes; methylimidazole and toluene, reflux for 2 d for P_6-Im-Me; (v) TMSBr, Et_3N, and toluene, room temp., 48 h.

The $\mathbf{P_6}$ materials were prepared from chlorobenzyl triethoxysilane using our recently published procedure,[11] and they showed the same characteristics. The $\mathbf{P_3}$ compounds were prepared from benzylimidazole triethoxysilane by a adapting a procedure typically used for the synthesis of imidazole-containing materials:[14] 1-[4-(trimethoxysilyl)-benzyl]imidazole (**1**, 1 equiv.) and tetraethyl orthosilicate (30 equiv.) were added to an aqueous ammoniac solution of monohydrated hexadecylpyridinium chloride, the latter being a structure-directing agent. The reaction mixture was heated at 80 °C for 48 h. The resulting suspension was filtered off and the surfactant removed by washing with an acidic ethanolic solution for 2 h yielding $\mathbf{P_3}$ (see experimental section for details). The $\mathbf{P_3}$ materials were characterized fully by several techniques, and transmission electron microscopy and small angle X-ray diffraction experiments revealed these materials to have a porous network with a 2D hexagonal arrangement of pore channels (Figure 1). The N_2 adsorption/desorption data recorded at 77 K exhibited a type-IV isotherm, which is characteristic of highly mesoporous materials. Furthermore the data showed the materials to have a monodispersed population of pores centered at ca. 3 nm (Figure 2), and a high surface area (A_{surf} = 933 m^2/g) and a large pore volume (V_p = 0.8 cm^3/g). Elemental analyses of $\mathbf{P_3}$ and $\mathbf{P_6}$ confirmed the incorporation of the organic precursor in the structures at a concentration of 0.5 mmol/g ($\mathbf{P_6}$: Cl 1.8 wt.-%, Si 37 wt.-%; found Si/Cl 27, expected for Si/Cl 30; $\mathbf{P_3}$: N 1.2 wt.-%, Si 40 wt.-%; found Si/N 16, expected for Si/N 15). The integrity of the functional groups within the materials was confirmed by solid state ^{13}C NMR spectroscopy (Figure S2). Moreover, the high-power decoupling (HPDEC) and cross-polarization magic-angle spinning (CP-MAS) ^{29}Si solid-state NMR spectra of $\mathbf{P_3}$ showed the following: (i) the high condensation of the material (from observation of two main signals

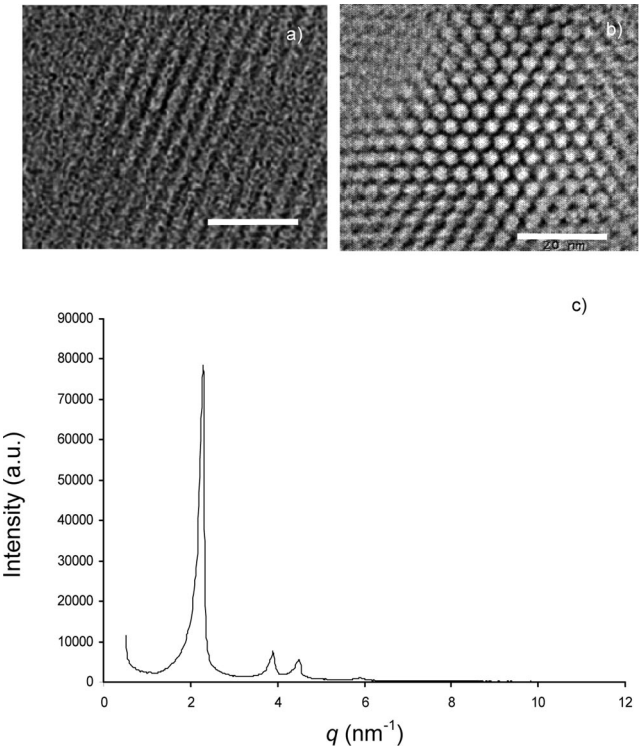

Figure 1. Data for P_3: (a) TEM micrograph (longitudinal), (b) TEM micrograph (transversal), (c) XRD pattern.

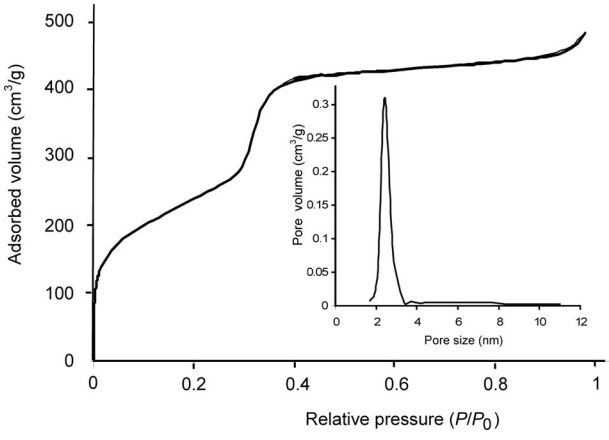

Figure 2. N_2 adsorption-desorption isotherm and pores distribution (inset) for $\mathbf{P_3}$.

at –102 and –111 ppm associated with Q^3 and Q^4 substructures, see Figure S3); (ii) the presence of one major surface organic species bonded to the inorganic matrix, mainly by three Si–O bonds (deduced from a signal at –78 ppm associated with T^3 substructures, along with a signal at –68 ppm associated with T^2 substructures, see Figure S4).

The **P_3** materials were transformed into imidazolium-containing materials by connecting methyliodide to the imidazole units, yielding **P_3-Im′-Me** materials (Scheme 1).

With regards to **P_6**, the imidazolium moieties were obtained by reacting **P_6** with methyl- or mesitylimidazoles,[15] using a procedure similar to one described recently,[11] to yield **P_6-Im′-Me** and **P_6-Im′-Mes**, respectively.

Hydrolysis with 2 M HX (where X = I for **P_3-Im′-Me**, and X = Cl for **P_6-Im′-Me** and **P_6-Im′-Mes**), followed by a drying step and a subsequent treatment with a TMSBr-Et_3N mixture or hexamethyldisilazane (HMDS) were performed on **P_3-Im′-Me**, **P_6-Im′-Me**, and **P_6-Im′-Mes** to transform the surface alkoxysilane and silanol groups into inert Si–$OSiMe_3$ moieties (passivation). The resulting materials, **P_3-Im-Me**, **P_6-Im-Me** and **P_6-Im-Mes**, were characterized fully using the aforementioned techniques (see Figures S8–S14 and ref.[11]). Finally, **P_3-Im-Me, P_6-Im-Me** and **P_6-Im-Mes** were converted to **P_3-Ir-Me**, **P_6-Ir-Me** and **P_6-Ir-Mes** by treatment with 1.5 equiv. of $AgOC(CF_3)_3$[16,17] in an acetonitrile/toluene (1:2) mixture (or in pure acetonitrile) at room temp. for 14 h to generate the corresponding Ag-carbenes (**P_3-Ag-Me**, **P_6-Ag-Me** and **P_6-Ag-Mes**), followed by a transmetallation step with $[Cp^*IrCl_2]_2$ (1 equiv.) at 60 °C for 24 h (Scheme 2).

The Ir–NHC-containing materials, namely **P_3-Ir-Me** and **P_6-Ir-Me/Mes**, were pale orange solids containing 8.08 wt.-% and 6.83 wt.-% of Ir, respectively. The ^{13}C CP-MAS NMR spectra of **P_6-Ir-Mes**, **P_3-Ir-Me**, and **P_6-Ir-Me** displayed signals corresponding to the respective organometallic units (see ref.[11], and Figures S16 and S22) and the following were also observed:

– For all the Ir-containing materials the signal for the CH_2 of the benzyl unit is observed at ca. 50 ppm, the aromatic carbons around 130 ppm, and the two peaks around 87 ppm (C_{sp2}) and 7 ppm (CH_3) are associated with the Cp* ligands.

– The signals for the methyl groups of the mesityl units are seen at δ = 30 and 18 ppm in the case of **P_6-Ir-Mes**.

– The signal for the methyl substituent of the NHC ligand is observed at δ = 37 ppm in the case of **P_6-Ir-Me**.

Moreover, the disappearance of the signal at δ = 140 ppm (attributed to the C atom at the 2-position of the imidazolium ring) and a N/Ir ratio of 2 are consistent with the conversion of imidazolium groupsto Ir–NHC units (> 95% yield). No signal corresponding to the carbenic carbon (Ir-CNHC) was observed due to the low concentration of surface species (0.0035 mmol/g of ^{13}C) and to the typical low intensity of such a quaternary carbon, especially in solid state NMR spectroscopy. Finally, the **P_3-Ir-Me**, **P_6-Ir-Me**, and **P_6-Ir-Mes** materials showed similar physical characteristics to their parent solids **P_3** and **P_6** (same pore network structures, similar porous texture with small pore diameters, surface areas, and pore volumes, due to surface protection groups).

The silylated and nonsilylated homogeneous Ir–NHC homologues of **P_3-Ir-Me**, **P_6-Ir-Me**, and **P_6-Ir-Mes**, namely, **C_{Si}-Ir-Me**, **C_{Si}-Ir-Mes**, **C-Ir-Me** and **C-Ir-Mes**, were synthesized via the same experimental pathway (Scheme 3): formation of the Ag–NHC complexes from the associated imidazolium compounds using $AgOC(CF_3)_3$, followed by a

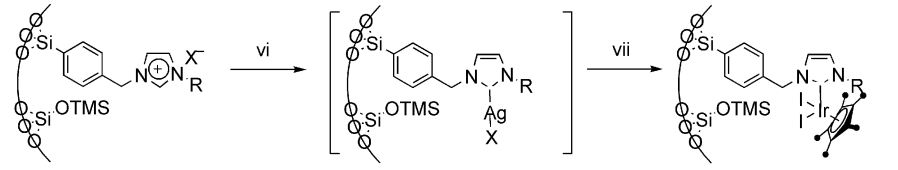

P_3-Im-Me: R = Me, X = I
P_6-Im-Me: R = Me, X = Cl
P_6-Im-Mes: R = Mes, X = Cl

P_3-Ag-Me: R = Me, X = I
P_6-Ag-Me: R = Me, X = Cl
P_6-Ag-Mes: R = Mes, X = Cl

P_3-Ir-Me: R = Me, X = I
P_6-Ir-Me: R = Me, X = Cl
P_6-Ir-Mes: R = Mes, X = Cl

Scheme 2. Synthesis of Ir–NHC carbenes inside the hybrid material using $AgOC(CF_3)_3$. Reagents: (vi) $AgOC(CF_3)_3$, CH_3CN, 14 h, r.t.; (vii) $[Cp^*IrCl_2]_2$, 24 h, 60 °C.

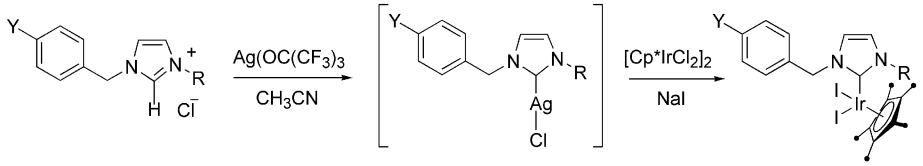

C-Im-Me, Y = H, R = Me
C_{Si}-Im-Me, Y = Si(O*i*Pr)$_3$, R = Me
C-Im-Mes, Y = H, R = Mes
C_{Si}-Im-Mes, Y = Si(O*i*Pr)$_3$, R = Mes

C-Ir-Me, Y = H, R = Me
C_{Si}-Ir-Me, Y = Si(O*i*Pr)$_3$, R = Me
C-Ir-Mes, Y = H, R = Mes
C_{Si}-Ir-Mes, Y = Si(O*i*Pr)$_3$, R = Mes

Scheme 3. Synthesis of the homogeneous analogues, **CSi-Ir-Me**, **CSi-Ir-Mes**, **C-Ir-Me** and **C-Ir-Mes** using the same synthesis methodologies used to prepare **P_3-Ir-Me**, **P_6-Ir-Me**, and **P_6-Ir-Mes**.

Table 1. H/D Exchange reaction results.[a]

Entry	Substrate	C-Ir-Me Conversion (%)		C-Ir-Mes Conversion (%)		P_3-Ir-Me Conversion (%)		P_6-Ir-Mes Conversion (%)		P_6-Ir-Me Conversion (%)	
		Initial (time)	Final (time)	Initial (time)	Final (time)	Initial (time)	Final (time)	Initial (time)	Final (time)	Initial (time)	Final (time)
1	acetophenone	99 (5 min)	–	98 (5 min)	–	56 (5 min)	95 (15 min)	54 (5 min)	94 (15 min)	59 (5 min)	95 (15 min)
2	9-acetylanthracene	90 (5 min)	98 (15 min)	58 (5 min)	97 (25 min)	17 (5 min)	97 (25 min)	12 (5 min)	92 (25 min)	17 (5 min)	96 (35 min)
3	benzophenone	20 (30 min)	60 (12 h)	19 (30 min)	59 (12 h)	14 (30 min)	28 (12 h)	12 (30 min)	28 (12 h)	–	–
4	diethyl ether	–	27 (12 h)	–	38 (12 h)	–	27 (12 h)	–	32 (12 h)	–	–

[a] Substrate (0.5 mmol), 2 mol-% of catalyst (based on Ir) and 4 mol-% of AgOTf in [D_4]methanol (2 equiv. based on Ir) were heated at 100 °C in a NMR tube equipped with a Young valve. The reaction mixture was monitored by ^{1}H NMR spectroscopy. A solution of ferrocene in $CDCl_3$ was used as an internal standard.

transmetallation step with $[Cp^*IrCl_2]_2$ in the presence of NaI. The resulting products were purified by silica-gel flash column chromatography, affording reddish brown solid crystalline compounds in high yields (85–95%). It is noteworthy that the addition of NaI to the reaction mixture during the transmetallation process yielded the corresponding iodide complexes, and afforded highly crystalline products when compared to the chloride homologues, and minimized the possibility of orthometallation as already mentioned by Peris et al.[7a] All the resulting Ir–NHC complexes were characterized by ^{1}H and ^{13}C solution NMR (Figures S23–S26) and HRMS. In the case of **C-Ir-Mes** and **C_{Si}-Ir-Me** the XRD structures were also solved (see ref.[11] and Figure 3, respectively).

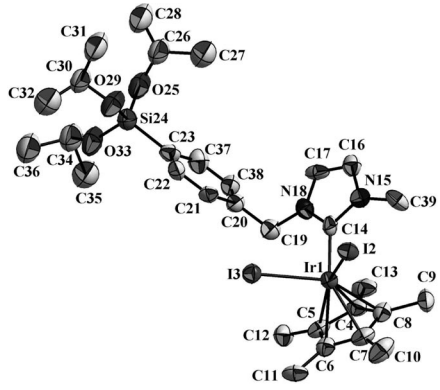

Figure 3. Crystal structure of **C_{Si}-Ir-Me** (CCDC-669230). Selected bond lengths for **C_{Si}-Ir-Me** are: Ir–C_{NHC} (2.02 Å), Ir–I (2.728 and 2.723 Å) and Ir–Cp*(centroid) (1.8425 Å).

Catalytic Activity

Catalytic H/D-exchange reactions were performed on three classes of substrates: methylarylketones (acetophenone, 9-acetylanthracene), benzophenone and diethyl ether using the following conditions: 2 mol-% of Ir–NHC complex, 4 mol-% AgOTf, in CD_3OD at 100 °C. Regardless of the catalyst used (homogeneous or heterogeneous), the activated substrates (acetophenone and 9-acetylantracene) are selectively deuterated at the methyl group (α-deuteration), and this deuteration is much faster (with 15 min) than that observed for nonactivated systems (diphenyl ketone and diethyl ether). In most cases (see Table 1, entries 1, 3 and 4), the heterogeneous catalysts need only slightly longer reaction times to achieve high conversion (> 90%) than their homogeneous equivalents. It is noteworthily that no H/D exchange reaction was observed when an Ir complex is not incorporated in the catalytic materials.[11]

The nature of the substituents on the NHC ligands has no influence on the catalytic performances of the Ir complexes, regardless of whether they were heterogeneous or homogeneous systems. Additionally, pore size had no impact on the activity of the heterogeneous catalysts. In particular, in the case of the bulky substrate 9-acetylanthracene (Table 1, entry 2), it is noteworthy that the substituents on the NHC units play a critical role in influencing the catalytic performances of the homogeneous and heterogeneous systems as determined from the substrate conversion after 5 min of reaction time: methyl-NHC shows faster conversion rates than mesityl-NHC, evidencing the influence of steric constrains on the transition state. In contrast, pore size does influence the catalytic activity of the heterogeneous systems, which is apparent when the activity of **P_3-Ir-Me** is compared with **P_6-Ir-Me**, were the only difference between these complexes is the substituents on the NHC ligand as mentioned above. This clearly indicates that there is no confinement effect, at least for these reactions, due to the decrease in pore size of the mesoporous catalysts investigated herein (Table 1). However, the sharp decrease in conversion rate on going from small to bulky substrate can be explained by a "local" confinement effect (first coordination sphere). This decrease in rate is further exacerbated in the case of the heterogeneous catalysts due to the proximity of the catalyst surface to the reaction site, which can affect the local environment (second coordination sphere).

Conclusions

To summarize, well-defined and single-site Ir–NHC-containing materials, and their corresponding homogeneous homologues, have been synthesized and characterized with the purpose of studying the factors that influence the C–H bonds activation of several classical substrates: pores diameters, local steric hindrance around the Ir metal center, and substituents on the NHC units. Two main conclusions can be drawn from this study: (1) the substituents on the NHC carbene ligand have the most important influence on the reaction rate in the case of large substrates; (2) in the case of heterogeneous systems, the major influence on the

rate of reaction is the nature of the first and second coordination spheres around the metal center (size of the NHC ligand, proximity of the active center to the surface due to the length of the tether and the size of the passivating $SiMe_3$ groups), but in these systems the rate is not correlated to the pore size, at least over the mesoporous size range investigated. This latter point suggests possible means for controlling the selectivity and the rate of catalytic reactions i. e. by modifying the local coordination sphere of a catalytic center (by altering the ligands, tether length, and surface functionalization) within a material, while keeping large pores for easy diffusion of substrate and product molecules.

Experimental Section

P_3-Im-Me: To **P_3-Im′-Me** (450 mg, 0.2 mmol) were added successively: toluene (15 mL), triethylamine (2 mL) and bromotrimethylsilane (0.5 mL, 3.2 mmol). After stirring the reaction mixture at 25 °C for 12 h, it was filtered, and the resulting solid was washed successively with toluene, methanol and diethyl ether. The resultant white solid was collected and dried under vacuum (135 °C, 10^{-5} Torr) for 14 h, which afforded 410 mg of **P_3-Im-Me**. ^{1}H NMR (500 MHz, solid state): δ = 0.12, 2.30, 3.02, 6.79, 7.70, 9.74 ppm. ^{13}C CP-MAS NMR (solid state): δ = 0, 18, 29, 32, 50, 117, 128, 135 ppm.

P_6-Im′-Me and P_6-Im-Me: The material **P_6** (300 mg) was treated with methylimidazole (4 mL) and the mixture was heated at 135 °C for 20 h. After filtration, the solid was washed successively with methanol, acetone, diethyl ether and then with ethanol with a Soxhlet. After drying under vacuum overnight (135 °C, 10^{-5} Torr), 280 mg of **P_6-Im′-Me** was obtained as a white material. The collected material was then suspended in 50 mL of 2 M aqueous HCl and stirred at 45 °*C* for 2 h. After filtration, the solid was subjected to several washings (3×50 mL of H_2O; 4×25 mL of acetone; 2×25 mL of diethyl ether), and drying (135 °C, 10^{-5} Torr, 12 h). Then the solid (250 mg) was suspended in toluene (10 mL) and treated with triethylamine (2 mL) and trimethylsilyl bromide (0.5 mL). After stirring for 24 h at 25 °C, the solid was collected by filtration, washed successively with methanol and diethyl ether, and dried overnight under vacuum (135 °C, 10^{-5} Torr), 270 mg of **P_6-Im-Me** was obtained. ^{1}H NMR (500 MHz, solid state): δ = 0.1, 1.7, 3.6, 7.0, 7.5 ppm. ^{13}C CP-MAS NMR (125.7 MHz, solid state): δ = –1, 12, 35, 53, 126, 134, 141 ppm.

P_3-Ir-Me: To a mixture of **P_3-Im-Me** (220 mg, 0.1 mmol) and $AgOC(CF_3)_3$ (55 mg, 0.16 mmol) was added acetonitrile (2 mL). The reaction mixture was stirred at room temp. under Ar in the absence of light for 12 h. Then $[Cp^*IrCl_2]_2$ (120 mg, 0.15 mmol) in acetonitrile (1 mL) was added dropwise to the reaction solution at room temp. The resulting reaction mixture was stirred for 24 h at 60 °C, filtered, and the solid collected and washed several times with acetonitrile, dichloromethane and methanol until the filtrate became colorless. Drying the solid for 12 h under high vacuum afforded 0.25 g of **P_3-Ir-Me** as a pale brownish solid. ^{1}H NMR (500 MHz, solid state): δ = 0.13, 1.53, 6.83, 7.70 ppm. ^{13}C CP-MASNMR (solid state): δ = 0, 6, 50, 59, 84, 117, 119, 127, 135 ppm. ^{29}Si CP MAS NMR (solid state): δ = 15, –68 (T^3), –77 (T^2), –100 (Q^3) and –108 (Q^4) ppm. Elemental analysis: Ir 8.08 wt.-%, Si 30.14 wt.-%.

P_6-Ir-Mes: Complex **P_6-Ir-Mes** was prepared from **P_6** according to a literature procedure.[11]

P_6-Ir-Me: Complex **P_6-Ir-Me** was prepared from **P_6-Im-Me** (270 mg, 0.12 mmol), $AgOC(CF_3)_3$ (62 mg, 0.18 mmol), and $[Cp^*IrCl_2]_2$ (60 mg, 0.06 mmol) in acetonitrile (2 mL) to yield 245 mg of **P_6-Ir-Me** as a brownish solid. ^{1}H NMR (500 MHz, solid state): δ = 0.1, 1.4, 3.6, 7.1, 7.9 ppm. ^{13}C CP-MAS NMR (125.7 MHz, solid state): δ = 0, 14, 37, 54, 64, 71, 89, 125, 133, 140 ppm.

Cp*Ir[3-benzyl-1-methylimidazol-2-ylidene]I_2 (C-Ir-Me). Representative Procedure: A mixture of $AgOC(CF_3)_3$ (128 mg, 0.37 mmol) and 1-benzyl-3-methylimidazolium chloride (52 mg, 0.25 mmol) in 3 mL of acetonitrile was stirred at room temperature for 2 h, and then $[Cp^*IrCl_2]_2$ (100 mg, 0.13 mmol) and NaI (150 mg, 1 mmol) were added to the solution. The mixture was heated at 60 °C and stirred for another 5 h. Then the reaction mixture was cooled to room temp., filtered through a pad of Celite, and then resulting mixture evaporated to give a brown solid. Purification by chromatography on silica-gel using a 2% acetone-heptane mixture afforded **C-Ir-Me** as a brown crystalline solid (163 mg, 87%). ^{1}H NMR (300 MHz, CD_2Cl_2): δ = 7.34 (m, 5 H, CH of the benzyl groups), 6.99 (d, J = 2.1 Hz, 1 H, N_{benzyl}–CH), 6.71 (d, J = 2.1 Hz, 1 H, N_{methyl}–CH), 6.20 (d, J = 15 Hz, 1 H, CH_2 of the benzyl groups), 4.95 (d, J = 15 Hz, 2 H, CH_2 of the benzyl groups), 4.00 (s, 3 H, N–CH_3), 1.81 (s, 15 H, CH_3 of the Cp* groups) ppm. ^{13}C{^{1}H} NMR (300 MHz, $CDCl_3$): δ = 151.9 (N_{benzyl}–CH), 136.7 (N_{methyl}–CH), 128–122 (C_{sp2} of the benzyl groups), 90.0 (C_{sp2} of the Cp* ligands), 58.1 (N–CH_2), 43.5 (N–CH_3), 10.6 (CH_3 of the Cp* ligands) ppm. HRMS (ES1$^+$): calcd. for $[Cp^*(NHC)IrI]^+$ ($[M - I]^+$) 625.08; found 625.08.

Cp*Ir[1-methyl-3-{4-(triisopropoxysilyl)phenyl}methylimidazolin-2-ylidene]I_2 (CSi-Ir-Me): The product was synthesized as described above for **C-Ir-Me** using 1-methyl-3-[{4-(triisopropoxysilyl)-phenyl}methyl]imidazolium chloride (42 mg, 0.11 mmol), $AgOC(CF_3)_3$ (60 mg, 0.17 mmol), $[Cp^*IrCl_2]_2$ (40 mg, 0.05 mmol) and NaI (50 mg, 0.34 mmol) yielding 90 mg of **CSi-Ir-Me** (94%) as a brown crystalline solid. ^{1}H NMR (300 MHz, $CDCl_3$): δ = 7.62 (d, J = 9.3 Hz, 2 H, CH of the benzyl groups), 7.25 (d, J = 9.1 Hz, 2 H, CH of the benzyl groups), 6.92 (d, J = 2.1 Hz, 1 H, N_{benzyl}–CH), 6.63 (d, J = 2.1 Hz, 1 H, N_{methyl}–CH), 6.02 (d, J = 15 Hz, 1 H, CH_2 of the benzyl groups), 5.21 (d, J = 15 Hz, 1 H, CH_2 of the benzyl groups), 4.23 (sep, 3 H, CH of the *i*Pr groups), 3.93 (s, 3 H, N–CH_3), 1.80 (s, 15 H, CH_3 of the Cp*), 1.17 (d, J = 6 Hz, 18 H, CH_3 of the *i*Pr groups) ppm. ^{13}C{^{1}H} NMR (300 MHz, $CDCl_3$): δ = 152.0 (N_{benzyl}–CH), 138.4 (C_{sp2} of the benzyl group), 135.2 (N_{methyl}–CH), 132.7–122.3 (C_{sp2} of the benzyl groups), 90.0 (C_{sp2} of the Cp* ligands), 65.4 (CH of the *i*Pr groups), 58.2 (N–CH_2), 43.5 (N–CH_3), 25.5 (CH_3 of the *i*Pr groups), 10.6 (CH_3 of the Cp* ligands) ppm. HRMS (ES1$^+$): calcd. for $[Cp^*(NHC)IrI]^+$ ($[M - I]^+$) 831.20; found 831.1.

Cp*Ir[3-benzyl-1-mesitylimidazol-2-ylidene]I_2 (C–Ir–Mes): This product was synthesized as described above for **C-Ir-Me** using 1-benzyl-3 mesitylimidazolium chloride (100 mg, 0.32 mmol), $AgOC(CF_3)_3$ (165 mg, 0.48 mmol), $[Cp^*IrCl_2]_2$ (127.5 mg, 0.16 mmol) and NaI (150 mg, 1 mmol) yielding 237 mg of **C-Ir-Mes** (87%) as a brown crystalline solid. ^{1}H NMR (300 MHz, CD_2Cl_2): δ = 7.46–7.34 (m, 5 H, CH of the benzyl groups), 6.90 (d, 1 H, $N_{mesityl}$–CH), 6.83 (s, 2 H, CH of the mesityl groups), 6.64 (d, 1 H, N_{benzyl}–CH), 6.27 (d, J = 15 Hz, 1 H, CH_2 of the benzyl groups), 4.78 (d, J = 15 Hz, 1 H, CH_2 of the benzyl groups), 2.31 (s, 3 H, CH_3 *para*), 2.04 (s, 6 H, CH_3 *ortho*), 1.75 (s, 15 H, CH_3 of the Cp* group) ppm. ^{13}C{^{1}H} NMR (300 MHz, CD_2Cl_2): δ = 175.2 ($C_{carbene}$), 147.8 ($N_{mesityl}$–CH), 138.6 (C_{sp2} of the benzyl group), 136.9 (N_{benzyl}–CH), 133.1–122.0 (C_{sp2} of the aromatic rings), 90.6 (C_{sp2} of the Cp* ligands), 58.5 (N–CH_2), 20.9 (CH_3 *para*), 18.5 (CH_3 *ortho*), 10.8 (CH_3 of the Cp* ligands) ppm. HRMS (ES1+): calcd. for $[Cp^*(NHC)IrI]^+$ ($[M - I]^+$) 731.1; found 731.15.

Cp*Ir[1-mesityl-3-{4-(triisopropoxysilyl)phenyl}methyl]imidazolin-2-ylidene]I_2 (CSi-Ir-Mes): This product was synthesized as described above for **C-Ir-Me** using 1-mesityl-3-[{4-(triisopropoxysilyl)-phenyl}methyl]imidazolium chloride (80 mg, 0.15 mmol), Ag-$OC(CF_3)_3$ (80 mg, 0.23 mmol), $[Cp^*IrCl_2]_2$ (60 mg, 0.075 mmol) and NaI (70 mg, 0.46 mmol) yielding a brown crystalline solid, **CSi-Ir-Mes** (138 mg, 84%). ^{1}H NMR (300 MHz, CD_2Cl_2): δ = 7.70 (d, J = 7 Hz, 2 H, CH of the benzyl groups), 7.48 (d, J = 7 Hz, 2 H, CH of the benzyl groups), 6.91 (d, J = 2.1 Hz, 1 H, $N_{mesityl}$–CH), 6.73 (s, 2 H, CH of the mesityl groups), 6.64 (d, J = 2.1 Hz, 1 H, N_{benzyl}–CH), 6.25 (d, J = 13 Hz, 1 H, CH_2 of the benzyl groups), 4.81 (d, J = 13 Hz, 1 H, CH_2 of the benzyl groups), 4.29 (sep, 3 H, CH of the *i*Pr groups), 2.32 (s, 3 H, CH_3 *para*), 2.06 (s, 6 H, CH_3 *ortho*), 1.75 (s, 15 H, CH_3 of the Cp* groups), 1.23 (d, J = 6 Hz, 18 H, CH_3 of the *i*Pr groups) ppm. $^{13}C\{^1H\}$ NMR (300 MHz, CD_2Cl_2): δ = 175.1 ($C_{carbene}$), 147.6 ($N_{mesityl}$–CH), 139.9 (Si–C_{sp2} of the benzyl group), 138.6 (N_{benzyl}–CH), 135.1–122.1 (C_{sp2} of the aromatic rings), 90.6 (C_{sp2} of the Cp* ligands), 65.5 (CH of the *i*Pr groups), 58.6 5 (N–CH_2), 25.3 (CH_3 of the *i*Pr groups), 20.9 (CH_3 *para*), 18.5 (CH_3 *ortho*), 10.8 (CH_3 of the Cp* ligands) ppm. HRMS (ES1+): calcd. for $[Cp^*(NHC)IrI]^+$ ([M – I]$^+$) 935.27; found 935.1.

H/D Exchange Reaction. Representative Procedure: Acetophenone (60 mg, 0.5 mmol), 2 mol-% of catalyst (based on Ir) and 4 mol-% of AgOTf in [D_4]methanol (10 mg, 2 equiv. based on Ir) were heated at 100 °C in a NMR tube equipped with a Young valve. The reaction mixture was monitored by ^{1}H NMR spectroscopy. A solution of ferrocene in $CDCl_3$ in a different sealed capillary tube was used as an internal standard. Conversion (%D) was measured by the relative disappearance of a peak at 2.5 ppm in the ^{1}HMR spectra, which corresponds to CH_3 group of acetophenone, and the appearance of peak at 4.8 ppm that corresponds to the OH group of CD_3OH.

Supporting Information (see also the footnote on the first page of this article): Full experimental details, Figures S1-S26 (solid-state ^{1}H, ^{13}C NMR and ^{29}Si spectra, small angle X-ray diffraction patterns and N_2 Adsorption/desorption isotherms for materials **P_3**, **P_3-Im′-Me**, **P_3-Im-Me**, **P_3-Ir-Me** and **P_6-Ir-Me**, and liquid state ^{1}H and ^{13}C NMR spectra of complexes **C-Ir-Me** and **CSi-Ir-Me**).

Acknowledgments

We thank Prof. A. Mehdi, Prof. C. Reyé and Prof. R. J. P. Corriu for fruitful discussions and technical assistance. This research was sponsored in part by the Agence Nationale de la Recherche, Programme Nanosciences et Nanotechnologies (ANR PNANO), project number ANR-05-NANO-034, and by the Agence Nationale de la Recherche, Programme Jeune Chercheuse/Jeune Chercheur (ANR JC/JC), project number ANR-05-JC-46372.

[1] W. A. Herrmann, *Angew. Chem. Int. Ed.* **2002**, *41*, 1290.
[2] R. H. Grubbs, *Tetrahedron* **2004**, *60*, 7117.
[3] S. Diez-Gonzalez, N. Marion, S. P. Nolan, *Chem. Rev.* **2009**, *109*, 3612.
[4] C. Samojlowicz, M. Bieniek, K. Grela, *Chem. Rev.* **2009**, *109*, 3708.
[5] E. A. B. Kantchev, C. J. O'Brien, M. G. Organ, *Angew. Chem. Int. Ed.* **2007**, *46*, 2768.
[6] R. H. Crabtree, *J. Organomet. Chem.* **2004**, *689*, 4083.
[7] a) R. Corberan, M. Sanau, E. Peris, *J. Am. Chem. Soc.* **2006**, *128*, 3974; b) C. M. Yung, M. B. Skaddan, R. G. Bergman, *J. Am. Chem. Soc.* **2004**, *126*, 13033; c) S. R. Klei, J. T. Golden, T. D. Tilley, R. G. Bergman, *J. Am. Chem. Soc.* **2002**, *124*, 2092.
[8] R. Corberan, M. Sanau, E. Peris, *Organometallics* **2006**, *25*, 4002.
[9] J. Atzrodt, V. Derdau, T. Fey, J. Zimmermann, *Angew. Chem. Int. Ed.* **2007**, *46*, 7744.
[10] I. Karamé, M. Boualleg, J.-M. Camus, T. K. Maishal, J. Alauzun, J.-M. Basset, C. Copéret, R. J. P. Corriu, E. Jeanneau, A. Mehdi, C. Reyé, L. Veyre, C. Thieuleux, *Chem. Eur. J.* **2009**, *15*, 11820.
[11] T. K. Maishal, J. Alauzun, J.-M. Basset, C. Copéret, R. J. P. Corriu, E. Jeanneau, A. Mehdi, C. Reyé, L. Veyre, C. Thieuleux, *Angew. Chem. Int. Ed.* **2008**, *47*, 8654.
[12] For seminal papers, see: S. L. Burkett, S. D. Sims, S. Mann, *Chem. Commun.* **1996**, 1367; D. J. Macquarrie, *Chem. Commun.* **1996**, 1961; D. Margolese, J. A. Melero, S. C. Christiansen, B. F. Chmelka, G. D. Stucky, *Chem. Mater.* **2000**, *12*, 2448; L. Mercier, T. J. Pinnavaia, *Chem. Mater.* **2000**, *12*, 188; R. J. P. Corriu, L. Datas, Y. Guari, A. Mehdi, C. Reyé, C. Thieuleux, *Chem. Commun.* **2001**, 763.
[13] For reviews, see: R. J. P. Corriu, A. Mehdi, C. Reyé, *J. Mater. Chem.* **2005**, *15*, 4285; F. Hoffmann, M. Cornelius, J. Morell, M. Fröba, *Angew. Chem. Int. Ed.* **2006**, *45*, 3216.
[14] B. Gadenne, P. Hesemann, J. J. E. Moreau, *Chem. Commun.* **2004**, 1768.
[15] A. J. Arduengo III, F. P. Gentry Jr., P. K. Taverkere, H. E. Simmons III, Patent number: US 6,177,575, Jan. 23, **2001**.
[16] A. Reisinger, N. Trapp, I. Krossing, *Organometallics* **2007**, *26*, 2096.
[17] A. Reisinger, D. Himmel, I. Krossing, *Angew. Chem. Int. Ed.* **2006**, *45*, 6997.

Received: June 22, 2010
Published Online: September 16, 2010

